materials proceedings

MDPI

Proceeding Paper

About Gas Permeability and Diffusion through Concrete †

Takwa Lamouchi [1,2], Severine Levasseur [3], Ludovic Potier [2], Thierry Dubois [2] and Frédéric Skoczylas [1,2,*]

[1] School of Civil Engineering and Architecture, Changzhou Institute of Technology, Changzhou 213032, China
[2] CNRS, Centrale Lille, UMR9013—LaMcube—Laboratoire de mécanique multiphysique et multiéchelle, Université de Lille, F-59000 Lille, France
[3] ONDRAF/NIRAS, RD&D-Department, Avenue des Arts 14, 1210 Bruxelles, Belgium
* Correspondence: frederic.skoczylas@centralelille.com
† Presented at the 10th MATBUD'2023 Scientific-Technical Conference "Building Materials Engineering and Innovative Sustainable Materials", Cracow, Poland, 19–21 April 2023.

Abstract: Gas production is expected in radioactive-waste storage structures. This will induce a slow increase in gas pressure, which necessitates the study of gas transfer at a low pressure. In this special case, calculations of the flow through storing materials while solely using permeability and Darcy's law are likely to be inadequate, as diffusion may play a crucial role in the process. The gas permeability and gas diffusion coefficient of industrial concrete have then been measured on the dry material. Diffusion tests were performed with a new device, specially designed for this study. The diffusion coefficient was directly measured with the use of the first Fick's law, as the test was analyzed under a steady state. Using some simplified hypotheses, it was then possible to compare the proportion of flow occurring due to diffusion with the one occurring due to permeation. The tendency is very clear and unambiguously shows that diffusion is predominant at a very low injection pressure but becomes negligible as soon as the gas pressure exceeds a moderate value.

Keywords: gas permeability; gas diffusion; dry concrete; injection pressure

Citation: Lamouchi, T.; Levasseur, S.; Potier, L.; Dubois, T.; Skoczylas, F. About Gas Permeability and Diffusion through Concrete. *Mater. Proc.* **2023**, *13*, 42. https://doi.org/10.3390/materproc2023013042

Academic Editors: Katarzyna Mróz, Tomasz Tracz, Tomasz Zdeb and Izabela Hager

Published: 7 March 2023

1. Introduction

Radioactive waste storage at great depths is likely to produce gas, mainly di-hydrogen, due to water radiolysis and corrosion. This will lead to gas transport through storage structures, such as concrete tunnels, or surrounding rocks—often clay rocks. This is why numerous studies were conducted by ONDRAF/NIRAS (in Belgium) or Andra (in France) in order to characterize the gas transfer properties of dry or partially saturated concrete or of its host rock. Gas-permeability tests are often carried out with a significant pressure gradient, i.e., with quite a high injection pressure—a few MPa, for example. It must be nevertheless mentioned that the gas pressure would slowly increase in the storage structure at the beginning of its production. As a consequence, and for the purpose of further simulations, it seems important to take this phase into account and to measure the respective role of permeation and diffusion in the gas-transfer process. Diffusion, which occurs when there is a gas concentration gradient, has in fact to be taken into account during the low-gas-pressure phase. Hence, the scope of the present experimental study was to design a gas-diffusion device and to evaluate the effective diffusion coefficient of the concrete intended to be used by ONDRAF/NIRAS (Organisme national des déchets radioactifs et des matières fissiles enrichies—in Belgium) for its storage tunnels. This measurement, conducted alongside 'traditional' permeability tests, demonstrates that a large proportion of gas transport may be occurring due to diffusion under a very low pressure injection.

2. Material and Sample Preparation

Concrete cylinders (around 140 mm diameter) cored from tunnel voussoirs of the HADES URL (the Belgian Underground research laboratory) were provided by ON-

DRAF/NIRAS. They were then re-cored into small rectified cylinders with a diameter of 65 mm and height of 50 mm. Such a height was considered to be enough for permeability and diffusion measurements, as it is more than three times the maximum aggregate size (14 mm). The concrete composition as provided by ONDRAF/NIRAS is presented in Table 1 below.

Table 1. Concrete composition.

Water kg/m^3	Cement CEM II/B-V kg/m^3	Fly Ash kg/m^3	Coarse Agg. (5–14 mm) kg/m^3	Fine Agg. (0–4 mm) kg/m^3
135	335	115	1252	540

Four samples were prepared, and their porosity was measured with the classical vacuum and weighing techniques [1]. The samples were dried at a temperature of 105 °C until the mass was constant. The results gave a mean porosity of 12.5%.

3. Experimental Setup and Experimental Conditions

Two different setups were used: one for permeability measurements and one for gas diffusion. Gas-permeability measurements are quite usual in our lab, and they did not require any new design. This was not the case with diffusion tests, which required the performance of a new design.

3.1. Gas Permeability

Most of the tests performed in the laboratory are 1D-flow-type tests on cylindrical samples (Figure 1). The gas pressure is P_1 at the upstream sample side and P_0 at the downstream side. Using Darcy's law and steady flow [2], we obtain:

$$P(x) = \sqrt{P_1^2\left(1 - \frac{x}{L}\right) + P_0^2\frac{x}{L}} \quad (1)$$

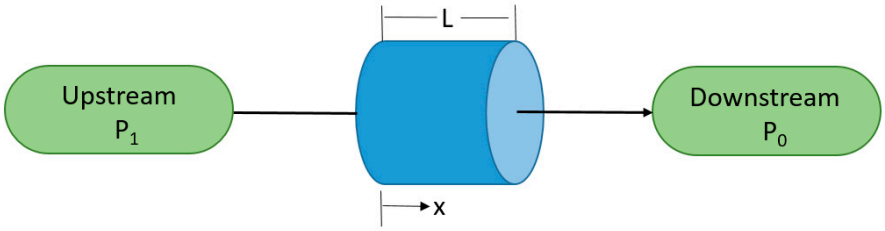

Figure 1. Schematic diagram of the steady-flow test method.

Q_1 is the volumetric gas flowrate at the upstream sample side [2]:

$$Q_1 = \frac{K_{app}A}{2\mu L}\frac{P_1^2 - P_0^2}{P_1} \quad (2)$$

K_{app} is the apparent gas permeability (apparent due to a potential Klinkenberg effect—see further), A is the sample cross-section, L is the sample length, and μ is the gas viscosity.

The flowrate Q_1 has to be measured to find the apparent gas permeability. Different methods can be used for this purpose: direct measurement with flowmeters (for example Brooks or Bronkhorst) or a measurement based on small pressure variation techniques (often used to calibrate the usual mass flowmeters). This second method was specially developed in our laboratory for materials with a very low permeability. Figure 2 presents a scheme of the system designed and used for this purpose.

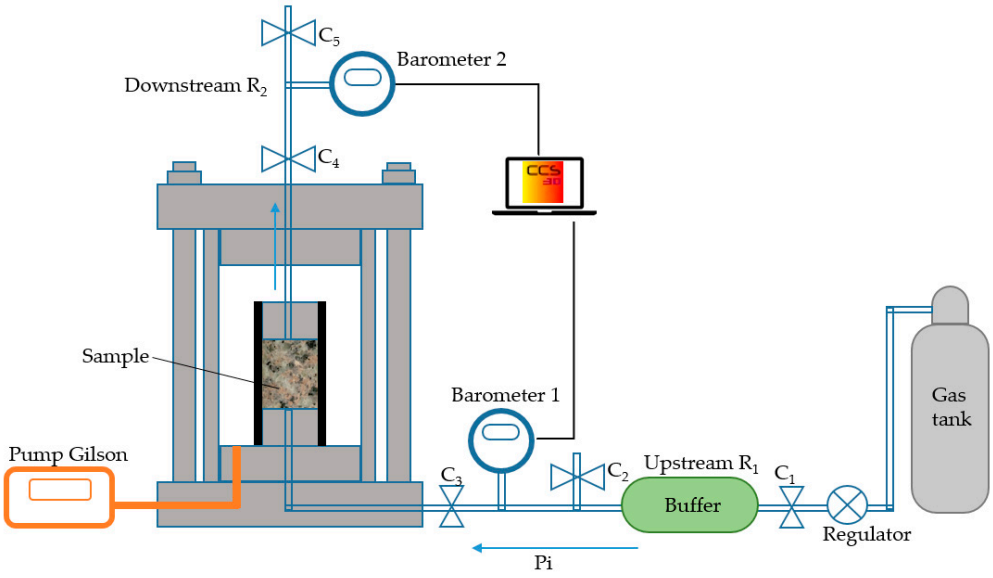

Figure 2. The device used for gas-permeability experiments.

The device is composed of a buffer reservoir R_1 and a tube reservoir R_2, respectively, connected at the upstream and downstream sample sides. The gas is first injected from a big gas tank at constant pressure P_1 (or P_i). The valve C_1 is closed as soon as a steady flow is assumed and R_1 is now feeding the sample with gas. The first possibility is then to measure the incoming flow rate Q_1. It is in fact the mean flowrate $Q_1{}^{mean}$ during a time Δt for which there is a decrease ΔP_1 of pressure P_1. Assuming that there is a steady flow during Δt at a mean injection pressure $P_1{}^{mean} = P_1 - \Delta P_i/2$, it can be easily shown [3] that:

$$Q_1^{mean} = \frac{V_1 \Delta P_1}{P_1^{mean} \Delta t} \quad (3)$$

The apparent permeability K_{app} can then be deduced from relation 2 in which $P_1 = P_1{}^{mean}$ and $Q_1 = Q_1{}^{mean}$. This method is called the quasi-steady flow method at high pressure because it is applied at the upstream sample side. Experiments were also conducted in the laboratory with electronic mass flowmeters when it was possible. They provided results that were compared to those given upstream by the quasi-steady method. The same results were virtually obtained with a difference in permeability of often less than 1%, as long as the ΔP_1 decrease did not exceed 5% of P_1.

V_1 is the volume of the R_1 reservoir, which includes the tubing volume between R_1 and the sample. This volume is obtained with an accurate calibration.

3.2. Diffusion Test—Principle of the Method

This test has been newly designed in our laboratory in order to induce gas transport through a concentration difference at atmospheric pressure on both sample sides. As the use of a gas spectrometer has caused some calibration difficulties, we chose to use a simpler gas analyzer with a 500 ppm resolution. This apparatus was calibrated to detect helium into nitrogen, and it can work in a closed circuit. This means that helium will diffuse into a reservoir containing nitrogen (initially 100% nitrogen) and that the apparatus will analyze a small proportion of the mix (nitrogen + helium) and re-inject this proportion into the reservoir after analysis. The principle of this test is indicated in Figure 3. There is a continuous pure helium flow at the upstream side. This implies that the helium concentration is constant at this side despite nitrogen diffusion.

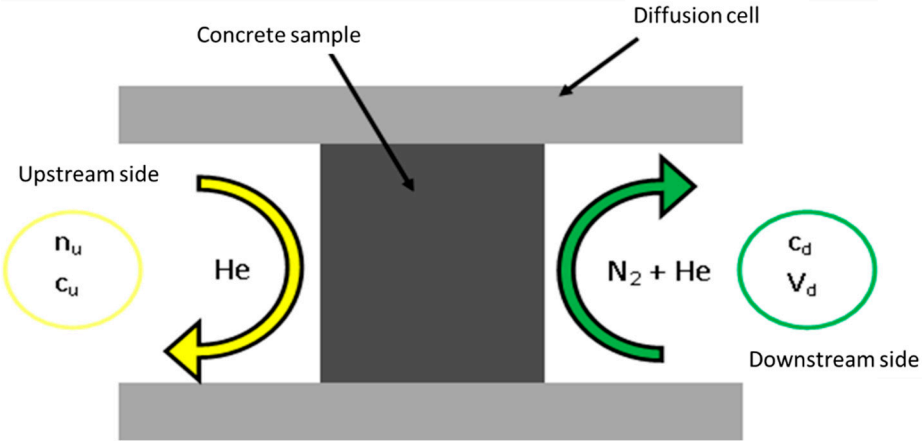

Figure 3. Schematic principle of the diffusion test; n_u is the number of helium moles, c_u and c_d are helium concentrations at the upstream (u) or downstream (d) sides, respectively. V_d is the downstream reservoir volume.

The device designed for diffusion tests is presented in the picture in Figure 4. The balancing device at Patm is realized by dip tubes whose height (into oil to avoid evaporation) can be adjusted. This allows for a pressure regulation with an accuracy that is better than one millibar. The percentage of helium at the downstream side is periodically measured by the gas analyzer.

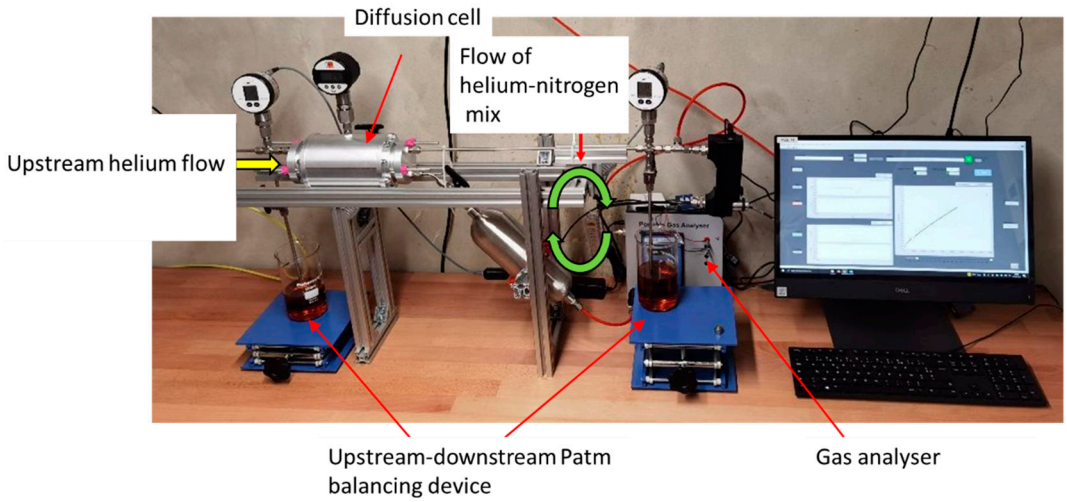

Figure 4. Picture of the device designed for diffusion.

3.3. Hypotheses and Test Analysis

By using some hypotheses, it is supposed that the diffusion process is controlled by the first Fick's law (1856), which, with a 1D geometry, gives:

$$J_x(x,t) = -D\frac{\partial c(x,t)}{\partial x} \quad (4)$$

J_x is the molar surface flow in $mol{\cdot}s^{-1}{\cdot}m^{-2}$;
D is the effective diffusion coefficient in $m^2{\cdot}s^{-1}$;
c is the gas concentration in $mol{\cdot}m^{-3}$.

The goal is then to measure J through the sample to obtain D under known or measured concentrations at the upstream and downstream sample sides. To be applied, Equation (3) needs a knowledge of the concentration 'c(x,t)' through the sample, which evolves with time. Under a constant molar flow J_x, the downstream concentration increases linearly with

time. At this stage, the mass balance equation coupled with Equation (3) leads to a linear concentration profile in the sample. This will be the main hypothesis used in the results.

The room temperature is constant and controlled at 22 °C or 295 K. Assuming that helium is a perfect gas (P_{atm} V = n_uRT), it is found that n_u = 40.8 moles per unit volume (1 m^3); thus, the concentration at the upstream side is c_u = 40.8 mol/m^3.

The molar flux through the sample cross-section will be:

$$\varphi(x,t) = J_x(x,t)\ A \tag{5}$$

φ molar flux through surface A in mol·s^{-1};
A sample cross-section in m^2.

For the calculations, it was supposed that the downstream helium concentration can be neglected in front of the upstream one, i.e., $c_d << c_u$. This leads to:

$$\frac{\partial c(x,t)}{\partial x} \approx \frac{-c_u}{L} \tag{6}$$

L is the sample length.

Under a stationary flow, 'p', the rate of helium particles' increase into the downstream reservoir, is directly linked to φ:

$$\varphi = p\ \frac{V_d}{V_m} \tag{7}$$

V_d downstream reservoir volume in m^3;
V_m molar volume (at P_{atm}) in m^3·mol^{-1};
'p' is in s^{-1}.

The following is thus obtained:

$$D = \frac{pLV_d}{Ac_uV_m} \tag{8}$$

with
$V_d = 1.09 \times 10^{-3}$ m^3;
$V_m = 24.05 \times 10^{-3}$ m^3·mol^{-1};
c_u = 40.8 mol·m^{-3}.

4. Results

4.1. Gas-Permeability Results

4.1.1. Results with Argon

Gas-permeability tests were performed with argon gas on dry material after the porosity measurements. Three injection pressures were used: 0.5, 1 and 1.5 MPa, in order to quantify the potential Klinkenberg effect [4]. This effect, also known as the 'slipping effect', may occur when the mean gas free path 'λ' is close to or lower than the mean pore size. As 'λ' is increasing when the gas pressure is decreasing, this effect is often visible on material with small pores (like concrete) and/or during tests with a weak injection pressure. As a result, if this effect is present, the measured permeability is apparent and higher than the intrinsic one. A very well-known correction was brought by Klinkenberg [4] in order to take this effect into account:

$$K_{app} = K_{int}\left(1 + \frac{\beta}{P_m}\right) \tag{9}$$

K_{app} is the apparent permeability (m^2);
K_{int} is the intrinsic permeability;
β is the Klinkenberg coefficient and P_m is the mean test pressure:

$$P_m = \frac{1}{L}\int_0^L P(x)dx \quad (10)$$

From relation (8), it can be seen that three different injection pressures are sufficient to assess and correct the Klinkenberg effect.

Two confining pressures (hydrostatic pressures) had been required by our partner ONDRAF/NIRAS: 2.25 and 4.5 MPa. Such a change in confining pressure can induce a significant permeability variation depending on whether the material is (micro-)cracked [3,5]. A typical result, obtained from sample OB-111, can be seen in Figure 5, and the whole set of intrinsic permeability results is presented in Table 2.

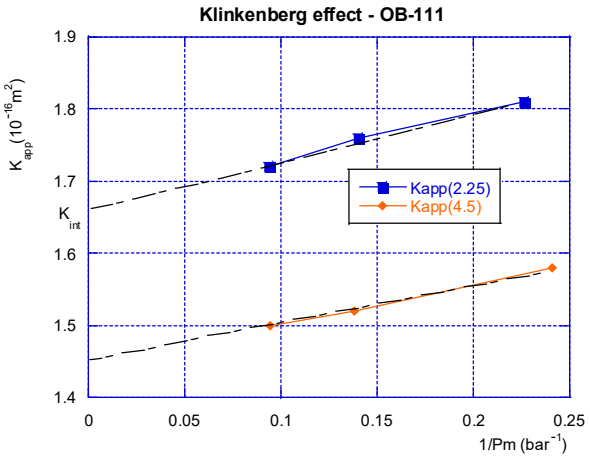

Figure 5. Example of Klinkenberg effect: tests performed at 2.25 or 4.5 confining pressure.

Table 2. Gas permeability results obtained with argon.

Sample	Confining Pressure (MPa)	K_{int} (10^{-16} m^2)	Coef. β (bar)
OB-111	2.25	1.66	0.4
	4.5	1.45	0.38
OB-121	2.25	1.73	0.31
	4.5	1.5	0.34
OB-321	2.25	1.57	0.28
	4.5	1.35	0.35
OB-422	2.25	1.37	0.31
	4.5	1.16	0.52

First of all, these results show a good material homogeneity in terms of its gas permeability. The confinement effect is very weak; this means that the material is not significantly cracked, as it is well known [6] that cracks close with a confining pressure, which in return induces a strong (and non-reversible) reduction in permeability. This is not the case here. The Klinkenberg effect is actually present but can be considered as being quite low.

4.1.2. Results with Helium

As mentioned before, the diffusion test will be performed with helium and not with argon. The results obtained will be used to evaluate the respective proportion of gas transfer due, respectively, to diffusion and permeation. It is thus important to compare the 'argon permeability' with the 'helium permeability'. One comparative set of tests was therefore performed on sample OB-422. The Klinkenberg effect is more sensitive with helium, as can be seen in Figure 6. This is consistent with the fact that the helium molecule size is lower than the argon molecule size [7]. 'β' is supposed to vary as 1/r, 'r' being the radius of the molecule. 'r' is three times higher for argon than for helium. This ratio (1/3) is more or

less respected by the 'β' coefficients presented in Table 3. On the other hand, it is clear that argon's and helium's intrinsic permeabilities are virtually the same, i.e., both can be used, without significant differences, to compare the respective flow resulting from permeation or from diffusion.

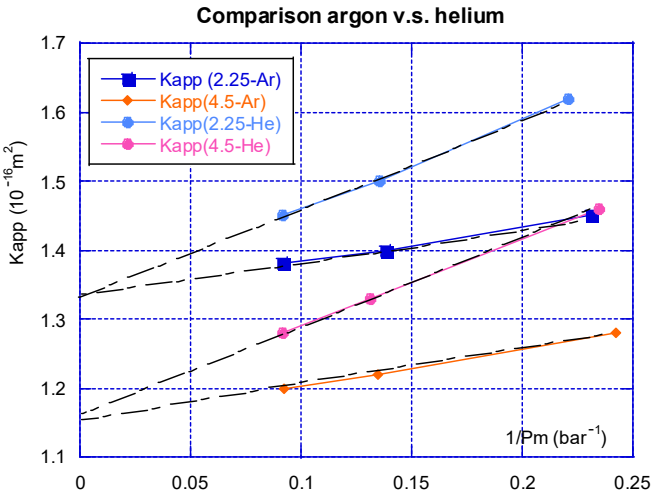

Figure 6. Permeability and Klinkenberg effect: argon vs. helium.

Table 3. Comparison of argon vs. helium.

Sample	Confining Pressure (MPa)	K_{int} (10^{-16} m^2)	β (Bars)
OB-422 Argon	2.25	1.33	0.38
	4.5	1.15	0.48
OB-422 Helium	2.25	1.32	1.02
	4.5	1.16	1.09

4.2. Gas-Diffusion Results

Helium-diffusion tests were carried out right after the permeability experiments. The downstream helium concentration is given in Figure 7. One can observe a very good homogeneity in these results for the four samples, as was also the case for the gas permeability. The four tests were performed at a 2.25 MPa confining pressure, as it was supposed that this pressure did not play a crucial role for permeability measurements. It is clear that, after around 3500 s, a permanent flow rate can be assumed, as the He concentration increases linearly. This provides evidence that for the dry concrete, the diffusion phenomenon is quite rapid. The slope 'p' (presented in §3.3) can be obtained from these results, allowing for the calculation of the diffusion coefficient 'D' with relation (7). The results are presented in Table 4; they lie within the range of the gas-diffusion coefficient often reported for concrete [8].

Table 4. Diffusion coefficient for the four samples.

Référence	p (s^{-1})	D ($m^2 \cdot s^{-1}$)
OB-111	2.5×10^{-6}	4.2×10^{-8}
OB-212	2.4×10^{-6}	3.9×10^{-8}
OB-321	2.6×10^{-6}	4.4×10^{-8}
OB-422	2.4×10^{-6}	3.9×10^{-8}

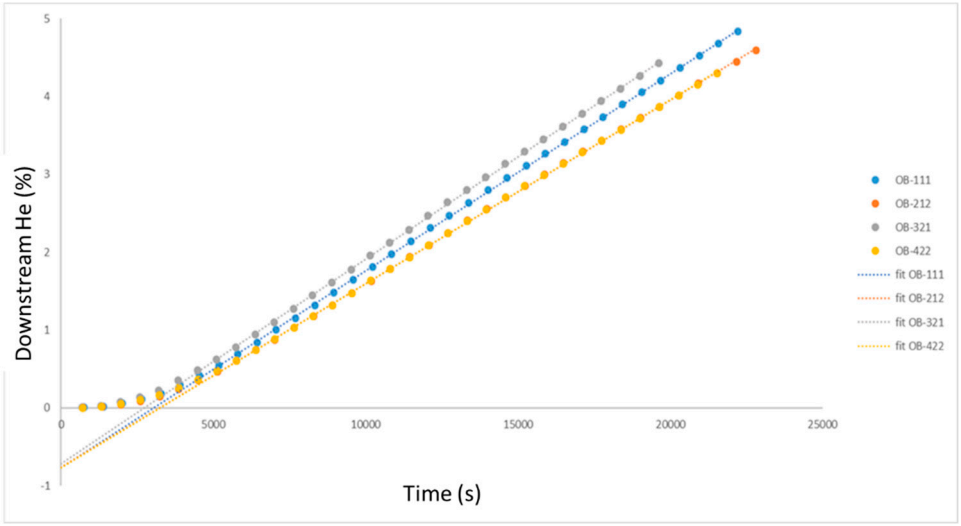

Figure 7. Helium proportion at the downstream side of samples.

4.3. Equivalent Permeability and Discussion

As mentioned before, the pressure due to gas production in a radioactive-waste storage should slowly increase. It is thus interesting to evaluate, in the case of a very low pression gradient, the proportion of gas transfer resulting from permeation and diffusion. This calculation was made within some simplified hypotheses. In particular, it was assumed that the diffusion coefficient does not depend on the gas pressure, which is not the case. The first step is to calculate the equivalent permeability due to diffusion. If an experiment is conducted with the gas pressure (pure helium, for example) at injection pressure P_1 (upstream sample side) and the drainage pressure at P_0 = Patm (air), it is supposed here that the diffusion coefficient helium-air is almost the same as for helium-nitrogen. If the test is interpreted as a permeability test, the downstream volumetric flowrate Q_0 is given by:

$$Q_0 = A\frac{K}{2\mu L}\frac{\left(P_1^2 - P_0^2\right)}{P_0} \tag{11}$$

This is linked to the number of moles per second n_k:

$$n_k = \frac{Q_0}{V_m} \tag{12}$$

In a diffusion test, this quantity is the same as φ mentioned before:

$$\frac{Q_0}{V_m} = n_k = \varphi = J{\cdot}A = D\frac{c_u}{L}A \tag{13}$$

The helium downstream concentration is still neglected, while the upstream concentration is:

$$c_u = n_u\frac{P_1}{P_0} \tag{14}$$

Then:

$$\frac{Q_0}{V_m} = D\frac{n_u}{L}A\frac{P_1}{P_0} = A\frac{K}{2\mu L}\frac{\left(P_1^2 - P_0^2\right)}{P_0}\frac{1}{V_m} \tag{15}$$

The equivalent permeability K_D can then be extracted from relation (15):

$$K_D = 2D\mu n_u V_m\frac{P_1}{\left(P_1^2 - P_o^2\right)} \tag{16}$$

As can be seen in relation (15), the equivalent permeability depends on the injection pressure P_1. K_D is roughly in the form $Cste/P_1$ when P_1 is increased. This means that the proportion of flow due to diffusion will be lesser and lesser as P_1 is increased. This is illustrated in Figure 8, which presents the ratio K_D/K, in which K has been chosen as a mean value of 1.5×10^{-16} m^2. This ratio is equivalent to the proportion of gas flow due to diffusion compared to the one due to permeation.

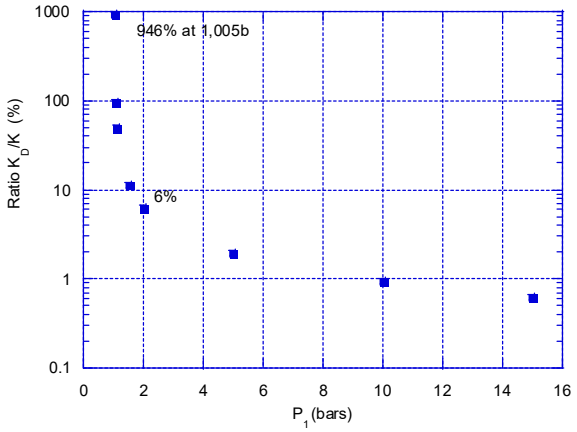

Figure 8. Flow ratio due to diffusion compared to the one due to permeation. P_1 is the absolute injection gas pressure.

5. Conclusions

A special device has been designed in order to measure gas diffusion through concrete (or other porous materials). The main goal of this study was to measure both the gas permeability and gas diffusion of an industrial concrete, which could be employed for tunnels intended for radioactive-waste storage. Gas production due to corrosion and water radiolysis should take place in these structures, and the low rate of production would first induce gas transfer at very low pressures, which are generally not used in gas-permeability experiments. Gas-permeability and diffusion tests were then performed on the same set of samples. They revealed that argon and helium permeability is virtually the same when corrected from a (slight) Klinkenberg effect. On the whole, gas permeability was found to be very homogeneous (order of magnitude of 1.5×10^{-16} m^2). This homogeneity was also verified for the effective diffusion coefficients (around 4×10^{-8} m^2/s). These coefficients were used to calculate an equivalent permeability K_D, which is dependent on the gas injection pressure. This clearly showed that under a low pressure gradient (or injection pressure), diffusion is largely predominant, whereas its induced flow can be neglected as soon as the injection pressure is larger than a few bars. This implies that gas diffusion must be taken into account at the beginning of gas production. Such a study should find a logical extension in the case of partially saturated concrete, which is likely to be encountered in 'in situ' structures.

Author Contributions: T.D., L.P. and F.S. conceived and planned the experiments. T.L. and L.P. carried out the experiments. T.L. and F.S. planned and carried out the analyses. S.L., T.L. and F.S. contributed to the interpretation of the results. F.S. and S.L. took the lead in writing the manuscript. All authors have read and agreed to the published version of the manuscript.

Funding: The publication cost of this paper was covered with funds from the Polish National Agency for Academic Exchange (NAWA): "MATBUD'2023-Developing international scientific cooperation in the field of building materials engineering" BPI/WTP/2021/1/00002, MATBUD'2023.

Acknowledgments: The authors thank ONDRAF/NIRAS for its technical and scientific support.

Conflicts of Interest: The authors declare no conflict of interest.

References

1. Andreola, F.; Leonelli, C.; Romagnoli, M.; Miselli, P. Techniques Used to Determine Porosity. *Am. Ceram. Soc. Bull.* **2000**, *79*, 49–52.
2. Zhang, D.; Agostini, F.; Jeannin, L.; Skoczylas, F. New Insights Brought by Micro-Tomography to Better Understand Gas Transfer Property Variation and Coupling Effects in Salt Rocks. *Rock. Mech. Rock Eng.* **2021**, *54*, 6457–6480. [CrossRef]
3. Chen, X.; Caratini, G.; Davy, C.A.; Troadec, D. Skoczylas, Coupled transport and poro-mechanical properties of a heat-treated mortar under confinement. *Cem. Concr. Res.* **2013**, *49*, 10–20. [CrossRef]
4. Klinkenberg, L.J. The permeability of porous media to liquids and gases. In *Drilling and Production Practices*; American Petroleum Institute: Washington, DC, USA, 1941; pp. 200–213.
5. Chen, W.; Han, Y.; Agostini, F.; Skoczylas, F.; Corbeel, D. Permeability of a Macro-Cracked Concrete Effect of Confining Pressure and Modelling. *Materials* **2021**, *14*, 862. [CrossRef] [PubMed]
6. Ding, Q.; Wang, P.; Cheng, Z. Influence of temperature and confining pressure on the mechanical properties of granite. *Powder Technol.* **2021**, *394*, 10–19. [CrossRef]
7. Degao, H.; Feng, Y.; Zhiguo, S.; Aiwei, Z.; He, Z.; Bin, L. Experimental study about the gas slip flow in Longmaxi shales from the southern Sichuan Basin. *Bull. Geol. Sci. Technol.* **2021**, *40*, 36–41. [CrossRef]
8. Sercombe, R.; Vidal, C.; Gallé, F. Adenot, Experimental study of gas diffusion in cement paste. *Cem. Concr. Res.* **2007**, *37*, 579–588. [CrossRef]